pH Effects on Molecular Adsorption and Solvation of p-Nitrophenol at Silica/Aqueous Interfaces

ARTICLE *in* THE JOURNAL OF PHYSICAL CHEMISTRY A · MAY 2013

Impact Factor: 2.69 · DOI: 10.1021/jp400482v · Source: PubMed

2 AUTHORS, INCLUDING:

Brittany Lauren Woods
University of Wisconsin–Madison
4 PUBLICATIONS **18** CITATIONS

THE JOURNAL OF PHYSICAL CHEMISTRY A

Article

pubs.acs.org/JPCA

pH Effects on Molecular Adsorption and Solvation of *p*-Nitrophenol at Silica/Aqueous Interfaces

B. Lauren Woods and Robert A. Walker*

Department of Chemistry and Biochemistry, Montana State University, Bozeman, Montana 59717, United States

Supporting Information

ABSTRACT: Resonance-enhanced second-harmonic generation (SHG) was used to examine the effects of solution pH and surface charge on *para*-nitrophenol (pNP) adsorption to silica/aqueous interfaces. During the early stages of monolayer formation, SHG spectra of interfacial pNP showed a single resonant excitation wavelength at approximately 313 nm regardless of solution pH. This resonance wavelength of adsorbed species is lower than the 318 nm excitation maximum of pNP in bulk aqueous solution. Experiments were performed at pHs of 1.0, 5.0, 7.0, and 10.5. Under these conditions, the silica surface carried a surface charge that ranged from slightly positive (pH = 1) to strongly negative (pH = 10.5) due to protonation/deprotonation of surface silanol groups. Over the course of 1−3 h, SHG spectra of pNP evolved so that spectra from interfaces fully equilibrated with solution pH showed two clear resonance features with wavelengths of approximately 310 and 330 nm. These wavelengths imply that adsorbed pNP samples two discrete local solvation environments at the silica/aqueous interface. On the basis of the solvatochromic behavior of pNP in different bulk solvents, the shorter-wavelength feature corresponds to a local environment having an effective dielectric constant of 9.5 (similar to that of dichloromethane), while the longer-wavelength feature lies outside of pNP's standard solvatochromic window. This longer-wavelength result implies an effective dielectric constant greater than that of bulk water or an adsorption mechanism that has pNP adsorbates sharing a proton with surface silanol groups (and adopting an electronic structure that begins to resemble that of its deprotonated form, *p*-nitrophenoxide). The longer-wavelength feature is weakest in the low-pH systems when the surface is either neutral or slightly positively charged and most prominent at the negatively charged silica/aqueous (pH = 10.5) interface. pNP adsorption isotherms for all systems showed approximate Langmuir behavior. Using concentration-dependent data from both low and intermediate pH led to calculated adsorption energies of −19 ± 2 kJ/mol for all pH values except pH 10.5 where ΔG_{ads} was −6 ± 2 kJ/mol. Taken together, these spectroscopic and adsorption studies of pNP adsorption to silica/aqueous interfaces as a function of aqueous pH show that interfacial acid/base chemistry can require hours to reach equilibrium and that the silica surface presents hydrogen-bonding solutes such as pNP with two distinct adsorption sites. The invariance of pNP's SHG spectra to bulk solution pH suggests that pNP solvation is dominated by substrate−solute interactions, with the adjacent solvent having very little influence on adsorbed solute properties.

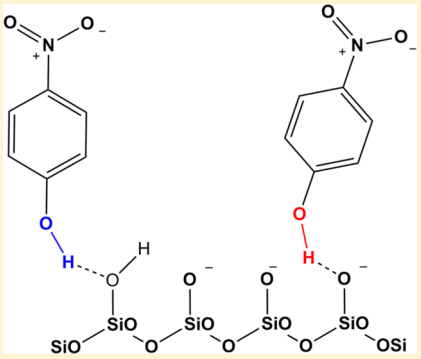

INTRODUCTION

Molecular adsorption at solid/liquid interfaces depends on a subtle balance between solute−solvent, solute−substrate, and substrate−solvent interactions. Understanding how each of these associations contributes to the overall affinity of a solute for different solid/liquid interfaces has far-reaching consequences for phenomena as diverse as adhesion,[1,2] biomineralization,[3−5] chromatographic separation,[6] and heterogeneous catalysis.[7] In order to predict whether or not solutes will adsorb to a solid/liquid interface and what sort of environment an adsorbate will experience at this boundary, one must know adsorption and solvation energies of both the solute and the solvent as well as how the anisotropy intrinsic to the interface changes solvent properties relative to bulk solution limits.[8] Furthermore, all of these quantities must be known accurately because determining whether or not solutes are surface-active requires evaluation of small differences between what can be large numbers. This task becomes even more challenging when the solvent structure at the surface can be affected by specific solvation forces such as hydrogen bonding[9] and nonspecific forces arising from surface charge[10−12] (Figure 1).

Many models have been developed to explore adsorption mechanisms.[13−17] Although these models have helped cultivate our understanding of interfacial behavior, they typically consider only a subset of the forces responsible for molecular adsorption to solid/liquid interfaces. Some studies focus primarily on adsorbate−substrate interactions,[16,17] while other work treats more rigorously the energetics and structure of solvent−substrate interactions.[13,14] In order to adsorb to an interface, a solute's association with the surface and surrounding solvent must be more energetically favorable

Special Issue: Prof. John C. Wright Festschrift

Received: January 15, 2013
Revised: May 5, 2013
Published: May 8, 2013

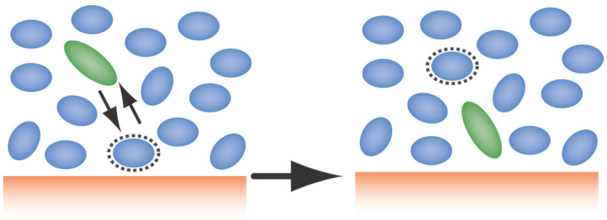

$$\Delta G_{tot} = \Delta G_{ads,u} - \Delta G_{solv,u} + \Delta G_{solv,v} - \Delta G_{ads,v} + \Delta G^*$$

Figure 1. A schematic representation of molecular adsorption to the solid/liquid interface. The total change in system free energy (ΔG_{tot}) must take into account association between the solute (u) and substrate ($\Delta G_{ads,u}$), the (partial) loss of solvation energy as the solute loses some of its solvation sphere ($-\Delta G_{solv,u}$), the loss of adsorption energy between the displaced solvent (v) and substrate ($\Delta G_{ads,v}$), and the gain in solvation energy as the displaced solvent resolvates in bulk solution ($\Delta G_{solv,v}$). ΔG^* accounts for nonadditive changes in interfacial solvent properties induced by the substrate. (See ref 8 for more details.)

than remaining solvated in bulk solution. With regards to silica/aqueous interfaces, the subject of this work, X-ray methods such as X-ray absorption near edge spectroscopy (XANES)[18] and X-ray photoelectron spectroscopy (XPS)[13] and theory have provided molecular-level insight into substrate and interfacial solvent structure, and some studies have explored how this structure changes as a function of pH.[10,19−21] Other techniques including optical and potentiometric methods have also examined water structure at silica and other mineral surfaces as a function of pH,[8,12,13,19,21,22] However, none of these studies have addressed specifically how changes in solvent structure and surface charge affect the tendency of solutes to adsorb to the interface nor have experiments examining the silica/aqueous interface clarified how the local environment surrounding adsorbed solutes differs from bulk solution limits.

At pH < 2, silica's surface silanol groups are fully protonated, with some silanol groups carrying an additional proton (as $-SiOH_2^+$), and the surface has a small positive charge. Deprotonation of the terminal silanols occurs at high pH, creating a net negative surface charge.[22−25] The potential of zero charge for silica/aqueous interfaces has been reported for aqueous pH between 2 and 4.[25,26] While different studies report differences in the quantitative acid/base properties of silica surfaces, most find that silica's surface acidity is characterized by two pK_a values, one that is slightly acidic (pH ≈ 5) and one that is more basic (pH ≈ 8).[22,24] Nonlinear optical studies reported by Ong et al. show strong enhancement of the second-order polarization by the static electric field from the charged surface. SHG data showing enhancement of the nonresonant second-order susceptibility pass through two equivalence points, one with a pK_a of 4.5 and another at a pK_a of 8.5.[22] On the basis of the magnitude of these changes, the authors conclude that the more acidic pK_a accounts for 19% of the surface silanol groups, while 81% of the surface silanol groups are characterized by the more basic pK_a. Potentiometric titrations performed by Meties and co-workers[24] report that 15% of the terminal silanol sites had a pK_a of 5.5, and the remaining 85% had a pK_a of 9.0. The authors further suggested that the acidic pK_a behavior of planar silica surfaces arises from isolated silanol groups, while the basic pK_a should be assigned to surface silanol groups that are hydrogen-bonded to neighbors[22] (Figure 2).

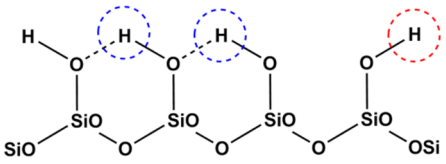

Figure 2. On the basis of nonlinear optical studies, Ong et al.[22] propose that the hydroxylated silica surface has two different silanol sites. One type of terminal silanol is hydrogen-bonded to neighbors (blue) and has a pK_a of 8.5. The other type of surface silanol is isolated (red) and has a lower pK_a of approximately 4.5.

More recent surface-specific, nonlinear optical experiments performed by Azam et al. tested the effects of the aqueous-phase ionic strength on the distribution of acidic and basic silanol groups.[27] The authors noted that the relative populations of −SiOH groups depended sensitively on the ionic strength and cation identity of different alkali halides dissolved in solution. The authors proposed that three-fold variation in the relative population of acidic silanol groups might be attributed to the effects of cations on the interfacial water structure. Modified water structure would, in turn, alter the acid−base chemistry of the silica surface. The authors correlated the fraction of ionized sites with hydrated cationic radii; cations with larger radii would induce more disruption in the interfacial water layer, an effect that would enhance the relative number of acidic silanol groups.

As pH increases, the terminal Si−OH groups become deprotonated. In the limit of high pH (≥ 10), silica surfaces become rough and more heterogeneous although such changes require exposure times of days or weeks.[28,29] Nevertheless, each of our experiments performed at high pH used new silica substrates. Given the chemical changes that occur at the silica/aqueous interface as a function of pH, one might expect interfacial solvation of adsorbed solutes to change also. To observe the effects of the aqueous-phase pH and surface charge on interfacial adsorption and solvation, experiments described below measure the affinity of *p*-nitrophenol (pNP) for the silica/aqueous interface and record the resonance-enhanced SHG spectra of the adsorbates at four different bulk pH concentrations. pNP is a solute having well-defined acid/base properties and solvatochromic behavior. pNP's solvatochromic window for electronic excitation extends from 288 nm in nonpolar, low dielectric solvents such as alkanes to 318 nm for polar solvents including DMSO and water. The fact that pNP's excitation wavelength in polar solvents is independent of hydrogen-bonding conditions shows that the solute's electronic structure is controlled exclusively by the surrounding dielectric properties rather than specific, localized solute−solvent interactions. With a pK_a of 7.2, pNP is almost exclusively neutral at low pH, but in basic conditions, pNP will be in its anionic form, *p*-nitrophenoxide (pNP^-). As an aqueous solution of pNP becomes more basic, the solution assumes a bright yellow color corresponding to a shift in the absorbance spectrum from λ_{max} of 317 nm (pH ≤ 5) to λ_{max} of 400 nm. (Figure 3) The relative amounts of pNP and pNP^- in solution as a function of pH can be calculated easily.

In the studies presented below, we investigate adsorption and solvation of pNP at silica/aqueous interfaces as a function of the solution-phase pH. Motivating this work is an extensive body of literature that has characterized the silica/aqueous interface in terms of solvent structure,[22,30] dynamics,[11,31] the effect of surface charge,[21,31,32] and the role played by these

dx.doi.org/10.1021/jp400482v | J. Phys. Chem. A 2013, 117, 6224−6233

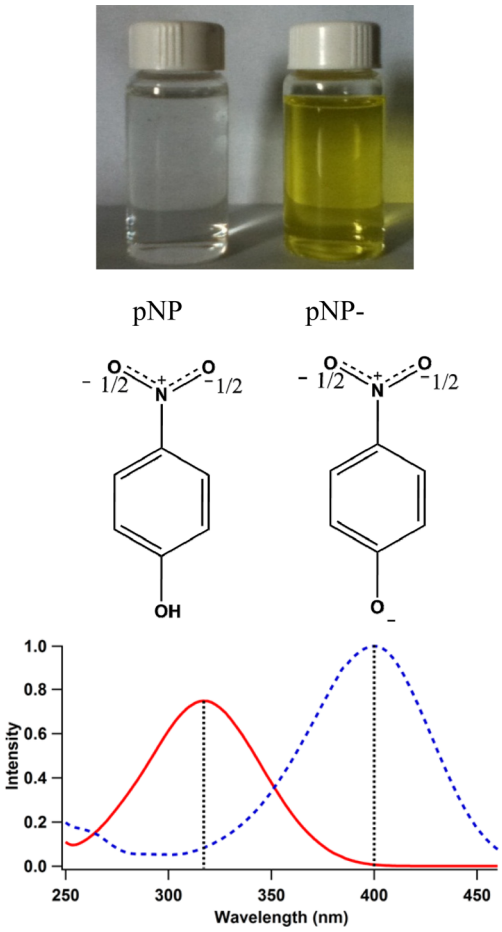

Figure 3. (Top) Comparison of pNP and pNP^-, ~2 mM of pNP in pH 1 (left) and pH 10.7 (right). (Middle) Structure of protonated and deprotonated pNP. (Bottom) UV/vis spectra of pNP in acidic conditions (red, solid line) and basic solution (blue, dashed line). When pNP is deprotonated, the electronic resonance wavelength shifts from 317 to 400 nm.

systems in analytical separation schemes.[2,5] Specifically, our studies seek to identify how (or if) molecular adsorption to silica/aqueous interfaces depends on interfacial charge and how interfacial charge affects interfacial solvation. In this context, the term "solvation" is used to describe the noncovalent interactions that a solute has with its surroundings, regardless of whether those interactions are with the solvent or the solid substrate.

Resonance-enhanced SHG spectra of pNP adsorbed to silica/aqueous interfaces proved to be time-dependent, with the SHG spectra changing shape over the course of hours. During the early stages of adsorption, spectra of interfacial pNP were characterized by a single excitation wavelength (313 nm), implying a single type of adsorption site. Furthermore, the approximate resonance wavelengths were largely pH-independent and reflected a local polarity more consistent with that of acetonitrile than with that of bulk aqueous solution. Over the course of 1−3 h, SHG spectra evolved to show two distinct excitation wavelengths, one at 310 nm and another at 330 nm. These data suggest that pNP adsorbed to fully equilibrated silica/aqueous interfaces samples two markedly different local dielectric environments. Silica surfaces are known to be highly heterogeneous,[28,29] but data presented in this work show how this heterogeneity directly impacts molecular adsorption and solvation. Furthermore, similarities between pNP spectra from the equilibrated silica/aqueous interface and the silica/vapor interface illustrate that the heterogeneity sampled by pNP depends almost exclusively on solute−substrate interactions. These results are discussed in the context of cooperative acid−base behavior between the solute and substrate and the importance of allowing for any long-time changes required to establish equilibrium at silica/aqueous interfaces.

EXPERIMENTAL METHODS

MP biomedical-grade pNP was purchased from Aldrich and used as received. Solutions of pH 1.0, 5.0, 7.0, and 10.7 (all ±0.2) were made using ACS-grade hydrochloric acid and 1 M sodium hydroxide solution (made from ACS-grade NaOH pellets). A PASCO Xplorer GLX data logger coupled with a PASPort high-resolution pH/ORP/ISE amplifier was used to monitor the solution's pH. In general, very small amounts of HCl and/or NaOH were needed to adjust the aqueous solution pH, and the ionic strength of these solutions was generally ≤10 μM. An exception to this behavior was the pH 1 aqueous solutions, where a significant amount of HCl was needed to lower the pH from 2.1 to 1.0. Buffers were not used to maintain the pH balance, thus requiring that all solutions be used immediately upon preparation. (Buffering solutes as well as high ionic strengths have been shown to affect solute adsorption in ways that can mask specific solute−substrate interactions.[27,32−34]) Silica slides were cleaned using a 50/50 sulfuric/nitric acid mixture and rinsed thoroughly with deionized water (Milipore, 18.2 MΩ, pH 5.5). The slide was then affixed in the sample cell in direct contact with the pNP containing aqueous solution and allowed to equilibrate for 1 or 3 hours.

The resonance-enhanced SHG signal was induced using a Libra-HE laser (Coherent, 85 fs pulses, 1 kHz repetition rate) coupled to a visible optical parametric amplifier (Coherent OPerA Solo) and collected using a PMT. Incident power before the sample ranged from 0.5 to 3.5 mW, with an average energy density of 1.38 mW/mm^2 at the sample surface. Additional details about this system can be found in earlier reports[35] and in the Supporting Information. Bulk optical absorbance data were recorded using a Hitachi U-3010 UV/vis spectrophotometer.

Resonance-enhanced SHG is a popular method used to study adsorption and interfacial solvation[8,35,36] and has been used to identify how surfaces change solvation environments from bulk solution limits.[35,37,38] Shifts in excitation wavelength describe the local polarity sampled by solvatochromic solutes at the silica/aqueous interface, and the strength of the solute's SHG signal is related to the population and average orientation of adsorbed solutes. The intensity of the SHG response, $I(2\omega)$, is related directly to the intensity of the incident light $I(\omega)$ through the induced second-order polarization $P^{(2)}(2\omega)$

$$I(2\omega) = |P^{(2)}(2\omega)|^2 = |\chi^{(2)}: E(\omega)E(\omega)|^2 = |\chi^{(2)}|^2 I(\omega) \quad (1)$$

where $P^{(2)}(2\omega)$ is the induced second-order polarization. $P^{(2)}(2\omega)$ is proportional to the system's second-order susceptibility, $\chi^{(2)}$, and the intensity of the incident field at frequency ω, $I(\omega)$. $\chi^{(2)}$ is a third-rank tensor that can be separated into resonant and nonresonant susceptibilities. The nonresonant (NR) susceptibility is intrinsic to any boundary where symmetry is broken and can reflect the behavior of the solvent and/or substrate but is inherently macroscopic. The NR

dx.doi.org/10.1021/jp400482v | J. Phys. Chem. A 2013, 117, 6224−6233

portion is typically assumed to be single-valued but can also be fitted to a linear function.[39,40] The resonant portion depends on properties of the adsorbates

$$\chi_r^{(2)} = N\langle\beta_{ijk}\rangle \qquad \beta = \frac{A}{\omega_0 - 2\omega - i\Gamma} \tag{2}$$

Here, A is a constant associated with the SH amplitude, ω_o is the resonant frequency of the transition, ω is the frequency of the incident light, and Γ is the line width. $\langle\beta\rangle$ represents the orientationally averaged molecular hyperpolarizability of interfacial adsorbates. Analysis of our spectroscopic data exploited all three of the molecular fitting parameters; ω_o served as a measure of the local polarity surrounding the adsorbed pNP, while Γ was interpreted in terms of the heterogeneity associated with the adsorption environment. In instances where SHG spectra showed two resonance features, the ratio of amplitudes (A_1/A_2) indicated the relative contributions from distinct adsorption sites.

Solute adsorption can be quantified with an adsorption isotherm. Assuming that the average orientation of the adsorbed pNP remains constant as a function of surface coverage, the square root of the SH intensity is proportional to the surface concentration. (eq 1) Plotting $I(2\omega)^{1/2}$ versus the bulk concentration, one can calculate adsorption energies after choosing an appropriate model. Isotherm data presented below were evaluated using several different models (including Freundlich, Langmuir–Freundlich, and Temkin fits)[41] but the quality of the fits did not unambiguously favor one model over another. Adsorption energies reported in this work are the result of fitting data to a Langmuir model despite the acknowledged limitations of Langmuir adsorption, namely, that surfaces must be homogeneous, that solutes behave ideally, and that the molecular adsorption ceases after a monolayer is formed.

In the Langmuir model (eq 3)

$$\frac{q}{Q} = \frac{bc}{1 + bc} \tag{3}$$

q is the adsorption capacity, Q is the maximum saturation capacity, b is a fitting parameter related to the adsorption energy, c is the bulk concentration, and the ratio of q/Q is proportional to the square root of the normalized signal. b can then be used in the following equation to solve for the free energy of adsorption (ΔG_{ads}) (eq 4)

$$b = e^{-\Delta G_{ads}/RT} \tag{4}$$

All fitting and data analysis was performed using Igor Pro v.6.02 (WaveMetrics, Inc.).

RESULTS AND DISCUSSION

To understand what role the aqueous solvent plays in controlling interfacial solvation of adsorbed pNP, we first measured the SHG spectrum of pNP adsorbed to the silica/vapor interface (Figure 4). To prepare this sample, a 4 mM solution of pNP in hexanes was allowed to equilibrate with a clean silica slide, and the hexanes were then allowed to evaporate. The silica slide with the adsorbed pNP was placed into the experimental assembly without any solvent present. While we acknowledge that the silica surface will retain some amount of adsorbed water vapor, we believe, based on data from silica/aqueous systems, that these silica–vapor data reflect primarily direct substrate–solute interactions. In the absence of a bulk aqueous phase, the pNP spectrum shows two peaks, one at 310 nm and the other at 330 nm. The appearance of two peaks implies that in the absence of a bulk solvent, pNP adsorbs to the surface through two different mechanisms, with the shorter wavelength feature indicating weaker interactions between the solute and substrate and the longer wavelength value indicating strong substrate/solute association.

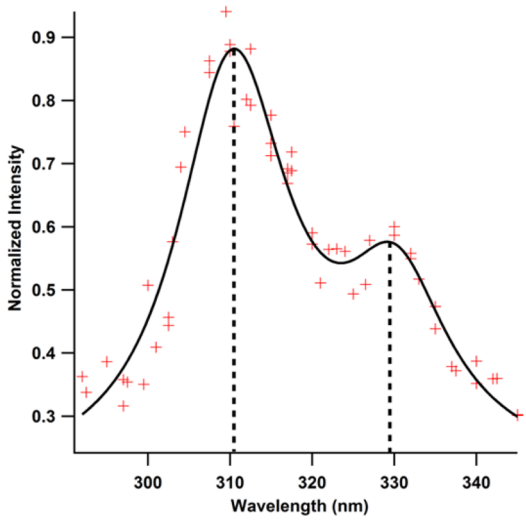

Figure 4. SHG spectrum for pNP at the solid/vapor interface. There are two peaks, one at 310 nm and a second peak at 330 nm. Additional details about the fitting parameters are reported in Table 2.

This two-site description of pNP adsorption to the silica/vapor interface also supports the studies cited above that found the acid/base properties of the silanol-terminated surface to be dominated by two distinct pK_a values. If hydrogen bonding between the pNP and surface silanol groups is the primary mechanism responsible for solute adsorption, then we assign the shorter-wavelength feature in the pNP SHG spectrum to pNP adsorbates donating hydrogen bonds to chemically resilient surface silanol groups, while the longer-wavelength feature is due to pNP donating hydrogen bonds to more negatively charged silanols (or "siloxides") such that the proton is shared more equally between the surface and pNP oxygen atoms. These assignments are based on careful analysis of changes in relative amplitudes of the two features at silica/aqueous interfaces as a function of aqueous-phase pH and are discussed in detail below.

In principle, pNP could also associate with the silica surface through dipole–dipole interactions between the surface silanol groups and pNP's $-NO_2$ group. pNP could also lie flat on the silica surface to promote interactions between the surface dipoles and the aromatic ring. Given the diffuse partial negative charge of pNP's $-NO_2$ group, however, coupled with unsuccessful efforts to fit the spectra with two populations of adsorbed solutes having oppositely phased contributions to the nonlinear susceptibility, we do not believe that pNP's $-NO_2$ group associates strongly with the silica surface (vide infra). Experiments measuring the orientation of pNP show that the approximate C_2 axis of the molecule lies ~75° off of surface normal, but this result does not change discernibly when data are acquired at 310 and 330 nm. (Orientation measurements and interpretation for several different systems are presented in the Supporting Information.) We note that these results are close to those reported originally by Higgins and Corn (70°) and suggest that the primary means of interaction between

dx.doi.org/10.1021/jp400482v | J. Phys. Chem. A 2013, 117, 6224–6233

adsorbed pNP and the silica surface involves hydrogen bond donation *from* the pNP *to* the surface silanol groups. A secondary interaction that would lead pNP to adopt an orientation that is almost parallel to the surface would be weaker hydrogen bond donation *from* the surface silanol groups *to* the pNP $-NO_2$ groups.

The first question to resolve when considering pNP adsorption to silica/aqueous interfaces is whether or not pNP adsorbs at all. pNP is moderately soluble in aqueous solution, with a solubility limit of 15.8 g/L (=0.11 M) and an octanol–water partitioning coefficient (log P = 1.91) that is relatively small compared to those of similarly sized aromatic solutes.[42] To assess pNP's affinity for silica/aqueous interfaces, the resonance-enhanced SH intensity ($I(2\omega)$) was recorded as a function of concentration. Plotting the square root of the signal as a function of pNP concentration allowed us to calculate ΔG_{ads} for the different silica/aqueous systems using eqs 3 and 4. One complication that we needed to take into account was that as the pH increases, the amount of pNP decreases due to deprotonation of the phenol to form the anionic phenoxide. Given a pK_a of 7.2, we calculated ratios of pNP/pNP$^-$ as a function of pH, and results are reported in Table 1. This effect

Table 1. Distribution, Adsorption, and Spectroscopic Data for pNP after a 1 h Equilibration Time[a]

pH	bulk conc. (mM)	pNP/pNP$^-$	peak wavelength (nm)	Γ (nm)	$-\Delta G$ (kJ/mol)
1.0	25	$10^{6.2}$	314 ± 2	37 ± 1	−21 ± 1
5.0	25	$10^{2.2}$	313 ± 2	37 ± 1	−17 ± 2
7.0	50	$10^{0.2}$	309 ± 3	44 ± 1	−17 ± 2
10.5	100	$10^{-3.3}$	316 ± 3	61 ± 1	−6 ± 2

[a]Values for the bulk solute concentration (=pNP + pNP$^-$), peak wavelength, line width (Γ), and adsorption energy (ΔG) as a function of pH following equilibration for 1 h. The ratio of pNP to its deprotonated form shows a decrease in pNP in favor of pNP$^-$ as the pH increases but affects neither the resonance wavelength nor adsorption energy. Increases in heterogeneity are indicated by increases in the line width.

was significant primarily for the high-pH experiments (at pH = 10.5) and, to a much lesser extent, for neutral pH (pH = 7). Our determination of ΔG_{ads} considered only the amount of neutral pNP in solution. Isotherms were measured after 1 h of equilibration for pH 10.5, 7, 5, and 1 (Figure 5). The values of ΔG_{ads} for these experiments are also reported in Table 1. Under acidic and neutral conditions, ΔG_{ads} remained relatively constant at −19 kJ/mol even as the silica surface began to accumulate a partial negative charge.[43] (The silica surface is neutral (and fully protonated) at a pH of 3–4. At higher pH, surface silanol groups will begin to deprotonate.)

As noted in the Introduction (Figure 1), the ∼−19 kJ/mol result represents a collective sum from many individual sources. From the SHG measurements, we cannot parse the contributions from these specific terms such as the cost of displacing water from the surface or the cost of partially desolvating pNP as it adsorbs. What the results do confirm, however, is that pNP adsorption to a silica/aqueous interface is thermodynamically favorable up to an aqueous pH of 7.

We note that at pH 10.5, the adsorption becomes markedly less favorable (ΔG_{ads} = −6 kJ/mol), a result that can be understood both in terms of competing equilibria between pNP adsorption and pNP/pNP$^-$ in bulk solution and the Coulombic

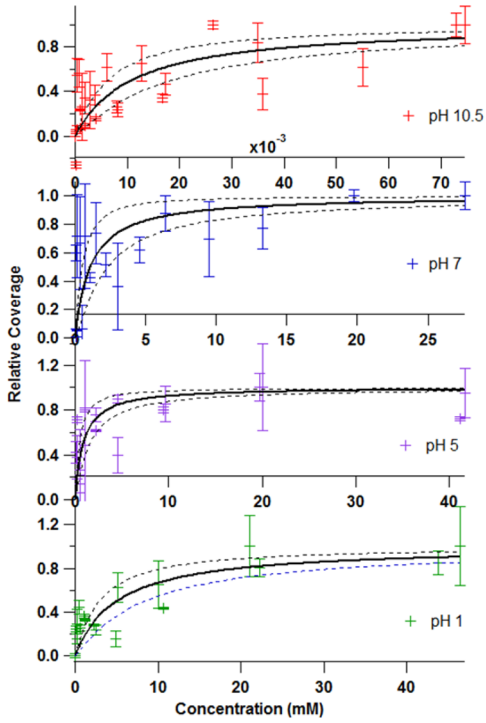

Figure 5. Isothermal data were collected at 315 nm with an equilibration time of 1 h for pH 10.5 (top), 7.0, 5.0, and 1.0 (bottom). All isotherms were fitted using the Langmuir fit, represented by a solid black line. ΔG_{ads} are reported in Table 1. The dashed lines correspond to 95% confidence limits in the fitted isotherm.

repulsion between the negatively charged silica surface and the negatively charged pNP$^-$ in solution. Given the molecular specificity of the SHG measurements (resonance enhancement is due to neutral pNP not anionic pNP$^-$), data are necessarily sensitive to adsorbed pNP but cannot discern the adsorption mechanism. In other words, these experiments cannot discriminate between the small number of neutral pNP solutes in solution adsorbing to the silica surface and negatively charged pNP$^-$ adsorbing to a surface silanol and formally sharing the proton. In this latter scenario, the adsorbate would acquire an electronic structure that more closely resembles that of the neutral solute rather than the anion. Regardless of pNP's origin to the silica/aqueous (pH 10.5) interface, the adsorption energy shows that neutral pNP adsorption is not as thermodynamically favored as it is at lower pH.

SHG spectra were recorded from silica/aqueous interfaces for aqueous solutions having pH concentrations of 1.0, 5.0, 7.0, and 10.5 (all ±0.2). Concentrations of pNP were chosen so that the surface would have full monolayer coverage. Spectra were acquired after allowing approximately 1 h for equilibration, and the data were fit to eqs 1 and 2 (Figure 6 and Table 1). (For the pH 7 and 10.5 solutions, we increased bulk pNP concentrations from 25 to ≥50 mM in order to obtain SH spectra having resolvable contrast between intensities on and off resonance.) The spectra are characterized by a single resonance feature that ranged from 309 (pH 7) to 316 nm (pH 10.5). Excitation wavelength maxima from the lower-pH systems fell between these two limits. The spectra show no systematic shift in resonance wavelength, and the line widths are broader than what one usually observes for solutes adsorbed to silica/liquid interfaces.[11,35,44] The data suggest that after ∼1 h, adsorbed pNP samples a single, heterogeneous environment

dx.doi.org/10.1021/jp400482v | J. Phys. Chem. A 2013, 117, 6224–6233

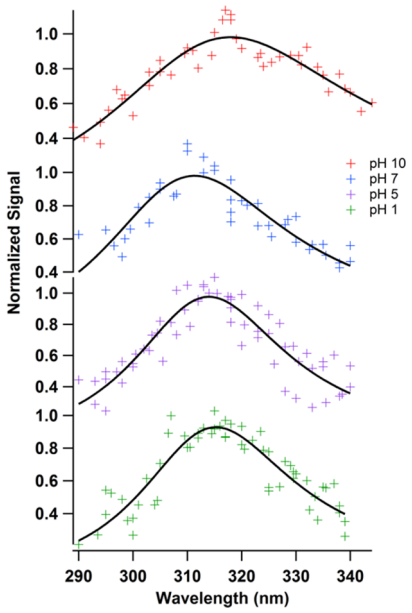

Figure 6. SHG data for pNP in increasing pH solutions (bottom to top). The resonance peak for all spectra was around 314 nm.

that is polar but slightly less polar than bulk aqueous solution. The line width broadens noticeably as the pH rises, leading us to conclude that the silica surface presents a more heterogeneous adsorption environment under more basic conditions. Adsorption energies ranged from −6 to −21 kJ/mol but did not show any systematic variation with $\lambda_{SH,max}$ or Γ.

The apparent insensitivity of spectroscopic features to aqueous pH and the dramatic differences between the silica/aqueous and silica/vapor spectra raise concerns that perhaps the silica surface is not fully equilibrated after allowing only 1 h of equilibration. To test the time-dependent condition of the silica surface as a function of pH, control experiments were performed to measure the nonresonant $\chi^{(2)}$ response of neat silica/aqueous interfaces as a function of pH but in the absence of a solute. As reported first by Eisenthal and co-workers, as the aqueous solution becomes more basic, the nonresonant SH field created at a silica/aqueous interface increases by more than an order of magnitude from pH 2 to 14, passing through two equivalence points at pH values of 4.5 and 8.5.[22] In our control experiments, the relative nonresonant SH intensities from the silica/aqueous interfaces at pH 1.0 and 10.5 were approximately equal after 1 h of equilibration. Only after 3 h did the SH response from the interface from the two different systems show the contrast comparable to that reported in ref 22. (Data from these experiments are presented in the Supporting Information.)

Precedent exists for believing that acid/base equilibration at silica/aqueous interfaces can require hours. Geiger and co-workers[32] have shown previously the effects that the aqueous solution ionic strength can have on the charged state of the silica/aqueous interface at various pHs. The authors explained their results in terms of strong ion−surface interactions that kinetically inhibit the interface's approach to equilibrium. Our experiments studying adsorption and solvation at silica/aqueous interfaces are performed with deionized water, but addition of either HCl or NaOH to create acidic or basic solutions, respectively, can lead to Na^+ or Cl^- concentrations as high as ∼0.3 M, comparable to concentrations used by Geiger and co-workers. Consequently, the specific "jamming" effects reported in ref 32 may play a role in explaining long equilibration times, although similar pNP behavior was observed under all pH conditions even when the ionic strength was quite low (e.g., pH = 5). The effects of specific adsorbed ions on molecular interactions with a silica substrate remain a subject still under investigation.

Figure 7 shows the SH spectra of pNP adsorbed to the silica/aqueous (pH7) interface after 1 and 3 h of equilibration.

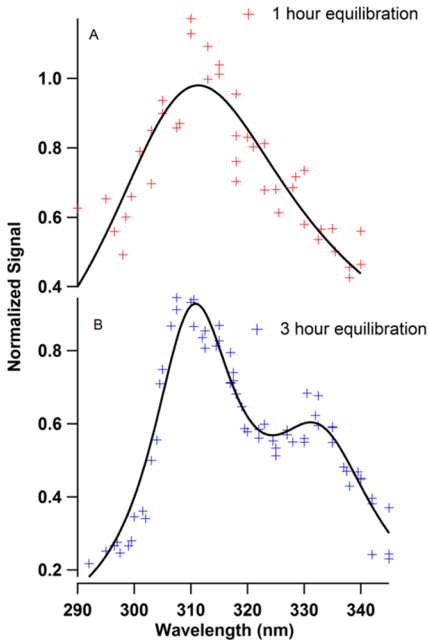

Figure 7. SHG spectra of 50 mM pNP adsorbed to the silica/aqueous interface from a pH 7 solution after a 1 h equilibration time (A) and 3 h of equilibration (B). Details about fitting parameters are described in the text.

(Spectra taken at even longer equilibration times show no change from the 3 h spectrum.) In contrast to the 1 h spectrum with a single electronic resonance, the 3 h spectrum shows two clear resonance wavelengths at 310 and 330 nm. These features match the wavelengths and line widths of the two resonances observed for pNP adsorbed to the silica/vapor interface (Figure 4). The amplitude ratios are different (with the silica/vapor spectrum having more relative amplitude in the shorter-wavelength feature) but are still within a standard deviation of each other. This result implies that once fully equilibrated, pNP adsorption and solvation at the silica/aqueous interface is largely independent of the surrounding solvent and surface charge state.

An alternative explanation for similarities between Figures 4 and 7 is that "nano"-bubbles are forming at the silica/aqueous pH 7 interface and that the 3 h SHG spectrum in Figure 7 actually represents measurement of sample pNP adsorbed to a silica surface with a microscopic vapor layer present. While possible, this explanation seems unlikely for several reasons. First, vapor formation (either through bubbles or a partial dewetting) is much more favored at hydrophobic solid surfaces, not the hydrophilic silica surfaces used in these experiments.[45,46] Second, bubble formation at (hydrophobic) surfaces from solutions saturated with CO_2 occurs on a ∼100−1000 s time scale, but the changes that we observe require hours.[45] Third, the tendency of aqueous solutions to form bubbles on basic surfaces is pH-dependent,[45] but we show below that

dx.doi.org/10.1021/jp400482v | J. Phys. Chem. A 2013, 117, 6224−6233

spectra acquired from silica surfaces in contact with pH 7 and 10.5 solutions are very similar. If a microscopic vapor phase were responsible for differences between early and long-time spectra, we also would expect to observe differences in the pH dependence between pH 7 and 10.5 conditions.

Furthermore, we propose that the emergence of two distinct adsorbed populations is the result of chemistry occurring at the interface rather than differences in the kinetics or thermodynamics associated with adsorption from bulk solution. Figure 8

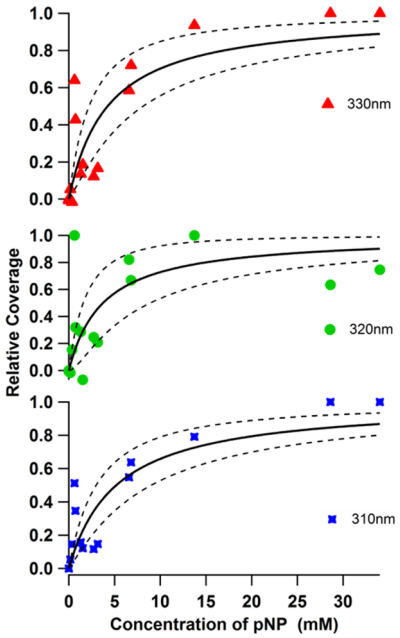

Figure 8. Isothermal data collected for pH 7 after 3 h of equilibration. Data were collected at the two resonant peaks (310 and 330 nm) along with 320 nm. The values of the ΔG_{ads} for 310, 320, and 330 nm data are −21 ± 1, −20 ± 3, and −21 ± 2 kJ/mol, respectively.

reports isotherm data acquired at three different wavelengths (310, 320, and 330 nm) for the silica/aqueous (pH 7) system measured after 3 h of equilibration. If one site were being populated preferentially or if nonresonant contributions to the second-order susceptibility were affecting the spectra through constructive or destructive interference, we would expect the 320 nm data to deviate significantly from the 310 and 330 nm data. Instead, however, isotherm data for all three wavelengths are virtually superimposable. From these results, we propose that the silica surface equilibrated with bulk solution presents pNP with two distinct solvation environments, one that is less polar than the bulk aqueous phase and one that is more polar. Furthermore, these sites arise following early time, nonspecific pNP adsorption followed by the surface becoming fully equilibrated with bulk solution pH and creating the two different sites. The distribution of these adsorption sites changes with aqueous-phase pH, suggesting that the two different adsorption sites are correlated with populations of neutral (−Si−OH) and deprotonated (−Si−O$^-$) silanol groups at the silica surface. The adsorption energies calculated from both the short- and long-wavelength features are equivalent.

Spectra of pNP adsorbed to all of the silica/aqueous interfaces were taken after 3 h and are shown in Figure 9. As with the pH 7 data, all spectra show evidence of two resonance wavelengths, although for the acidic silica/aqueous (pH 1) interface, the long-wavelength feature appeared only as a

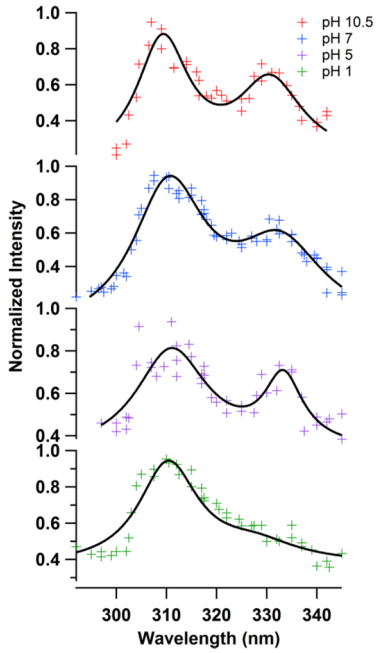

Figure 9. After 3 h of equilibration, the first peaks on all of the pH experiments are slightly blue-shifted from ∼315 to 310 nm. At 330 nm, a second peak is present in all of the experiments, although at pH 1, it can only be seen as a shoulder.

shoulder to the dominant resonance at 310 nm. Values for the resonance peak locations and line widths are reported in Table 2. The peak locations vary very little, implying that adsorbed pNP is sensitive primarily to local effects and not influenced significantly by bulk pH or by general properties such as the interfacial Helmholtz layer or Debye length.[41] When taking into account the behavior of the resonance amplitudes as a function of bulk solution pH, these observations suggest two different hydrogen-bonding mechanisms for the short- and long-wavelength resonances (Figure 10).

Also included in Table 2 are the A_1/A_2 ratios for the intensity amplitudes as a function of pH, where A_1 and A_2 are the amplitudes of the 310 and 330 nm features, respectively, as determined from fitting the data to eqs 1 and 2. A general observation is that at higher pH, the A_1/A_2 ratio is smaller, suggesting that the long-wavelength feature is associated with the deprotonated surface silanol groups. Data from the two acidic silica/aqueous systems (pH = 1 and 5) show large amplitude ratios, but these data also have a high degree of uncertainty associated with them. Fitting for acidic conditions were problematic and showed no strong preference for a specific parameter. Repeated efforts to fit the pH 5 spectrum lead to the following observations: amplitude fits are flexible, but line width and peak wavelengths tended to remain relatively consistent throughout the fitting process. We note that the quality of the fit for the pH 1 data is particularly poor and fails to capture the very sharp edge at short wavelengths. The origin of this effect is uncertain, although we note that only for the acidic system does the silica surface have a slight formal positive charge. However, efforts to include a third specific adsorption site with physically meaningful spectroscopic parameters did not improve the quality of either the pH 1 or 5 fits.

When reporting results from nonlinear optical spectra having two features reasonably close in resonance frequency, one needs to consider carefully the coherent contribution of each

dx.doi.org/10.1021/jp400482v | J. Phys. Chem. A 2013, 117, 6224−6233

Table 2. Data for pNP after a 3 h Equilibration Time and for the S/V Interface[a]

pH	bulk conc. (mM)	λ_1 (nm)	Γ_1 (nm)	λ_2 (nm)	Γ_2 (nm)	A_1/A_2
1.0	25	310 ± 1	14 ± 1	328 ± 5	38 ± 2	3 ± 2
5.0	25	311 ± 1	18 ± 1	333 ± 1	9 ± 1	2.2 ± 2
7.0	50	310 ± 1	16 ± 1	331 ± 1	19 ± 1	1.3 ± 0.2
10.5	100	309 ± 1	13 ± 1	331 ± 1	16 ± 1	1.2 ± 0.8
S/V	4	310 ± 1	17 ± 1	330 ± 1	16 ± 1	1.9 ± 0.6

[a]Values for the peak wavelengths, line widths (Γ), and the ratio of amplitudes for each spectrum in Figure 9. For comparison, the values from the solid/vapor experiment have also been included.

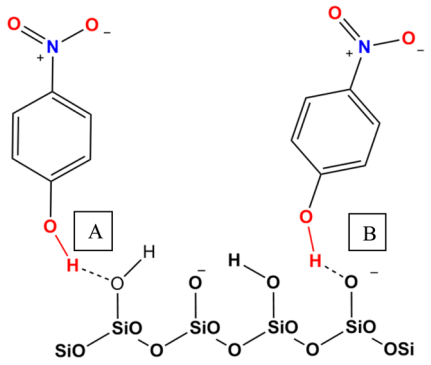

Figure 10. Schematic illustration representing the two populations associated with pNP adsorption to the fully equilibrated silica/aqueous interface. (A) The terminal silanol and pNP are both in their neutral forms and share a hydrogen. (B) As the surface becomes deprotonated, a negative charge is built up, and the second adsorption mechanism is assigned to pNP^- H-bonding to Si−OH or a deprotonated O^- bonding to a protonated pNP.

transition and the possibility that spectra may contain significant constructive or destructive interference from the two resonances with each other and/or with any nonresonant background. In spectra containing only isolated resonance features, interference between $\chi^{(2)}_{res}$ and $\chi^{(2)}_{NR}$ can lead to pronounced asymmetry with an extreme example being derivative-shaped resonance transitions such as those observed in nonlinear vibrational spectra of alkyl monolayers on metals.[47] Similar interferences have also been observed in SH spectra.[9,35,48,49] In the event that a SHG spectrum contains contributions from two adsorbate populations, constructive and destructive interference can result from both resonant terms of the $\chi^{(2)}$ tensor as well as the nonresonant contribution. Depending on the relative signs of the two resonant terms, line shapes may show constructive or destructive derivative-like behavior. The data in Figures 8 and 9 have been fit to eq 2 while considering all permutations of resonant and nonresonant $\chi^{(2)}$ contributions. To within the limits of experimental reproducibility, we believe that the spectra in Figure 8 all reflect contributions from two distinct populations of pNP sharing similar net orientations adsorbed to silica/aqueous interfaces. Furthermore, the effects of the nonresonant susceptibility, although nonzero, do not strongly affect the measured resonant behavior. One reason that the features in the 3 h spectra do not show strong evidence of interference is that the resonances are consistently narrower than those in the 1 h spectra. These findings imply that the two adsorption sites (illustrated schematically in Figure 9) at the fully equilibrated silica/aqueous interface are more homogeneous than the environment sampled after only 1 h of equilibration.

CONCLUSIONS

Summarizing the findings from our studies of pNP adsorption to silica/aqueous interfaces as a function of aqueous-phase pH, we conclude that while initial adsorption may occur indiscriminately, the resulting equilibration between adsorbed solutes and the silica substrate is neither simple nor rapid. Furthermore, interactions that adsorbed pNP solutes experience at the interface appear to be dominated almost exclusively by close association with the silica substrate with the aqueous solvent playing primarily a spectator's role. Specific observations from this work include the following:

- pNP adsorbed to the silica/vapor interface samples two distinctly different environments, with one characterized by weaker interactions (leading to a shorter-wavelength resonance in the SH spectrum) and one characterized by strong interactions between the solute and substrate that push the pNP resonance wavelength beyond the polar limit of the solute's solvatochromic window.
- Equilibration of adsorbed pNP at the silica/aqueous interface requires up to 3 h regardless of aqueous-phase pH.
- During the initial stages of adsorption, pNP samples a single albeit heterogeneous environment that is slightly less polar than the bulk aqueous solution given an observed shift in pNP's excitation to shorter wavelengths. If modeled using a Langmuir isotherm, pNP adsorption is thermodynamically favored with a ΔG_{ads} of ∼−20 kJ/mol except under alkaline conditions (pH 10.5) where ΔG_{ads} is −6 kJ/mol.
- Once fully equilibrated with the silica/aqueous interface, pNP samples two distinct environments, one polar and one nonpolar. While the nature of these two environments does not depend on bulk aqueous pH, their relative importance changes with changing pH. At low pH, pNP adsorbed to the less polar site makes a larger contribution to the SH spectrum, and at higher pH, contributions from the more polar site become more pronounced. These findings correlate with the two types of surface silanol groups reported to exist at the hydroxylated silica surface.

The silica/aqueous interface represents a complex, heterogeneous environment that creates different mechanisms for solute adsorption from aqueous solution. Furthermore, adsorbed solutes and the surface can require hours to equilibrate fully. Given the importance of molecular adsorption to silica surfaces in fields as diverse as geochemistry, separation science, and environmental remediation, a molecularly based understanding of solute−substrate interactions will require extensive and quantitative studies. Results presented in this work and elsewhere have begun to unravel some of the relevant issues (time, ionic strength, and pH) associated with chemistry occurring at the solid/liquid interface. Our findings and their implications motivate continued efforts to develop validated, predictive models that can accurately describe molecular adsorption to these ubiquitous and complicated boundaries.

dx.doi.org/10.1021/jp400482v | J. Phys. Chem. A 2013, 117, 6224−6233

■ ASSOCIATED CONTENT

Supporting Information

Plot of the nonresonant harmonic field, SHG spectra of pNP, SHG orientation spectra of pNP, and parameters for the experimental setup. This material is available free of charge via the Internet at http://pubs.acs.org.

■ AUTHOR INFORMATION

Corresponding Author

*Address: Rm 57, Dept. of Chemistry and Biochemistry, Bozeman, MT 59717. Phone: (406) 994-7928. E-mail: rawalker@chemistry.montana.edu.

Notes

The authors declare no competing financial interest.

■ ACKNOWLEDGMENTS

The authors would like to gratefully thank the NSF International Collaboration in Chemistry (ICC) program (CHE-1026870) for support. The authors thank Dr. Renee Siler for contributions toward the experimental setup and David Halat, who assisted with analysis and programing.

■ REFERENCES

(1) Escudero, C.; Salmeron, M. From Solid−Vacuum to Solid−Gas and Solid−Liquid Interfaces: In Situ Studies of Structure and Dynamics under Relevant Conditions. *Surf. Sci.* **2013**, *607*, 2−9.

(2) Weetall, H. H. Preparation of Immobilized Proteins Covalently Coupled through Silane Coupling Agents to Inorganic Supports. *Appl. Biochem. Biotechnol.* **1993**, *41*, 157−188.

(3) Chen, Z.; Li, Z.; Lin, Y.; Yin, M.; Ren, J.; Qu, X. Biomineralization Inspired Surface Engineering of Nanocarriers for pH-Responsive, Targeted Drug Delivery. *Biomaterials* **2013**, *34*, 1364−71.

(4) Mann, S. Molecular Techntonics in Biomineralization and Biomimetic Materials Chemistry. *Nature* **1993**, *365*, 499−505.

(5) Znidarsic, W. J.; Chen, I. W.; Shastri, V. P. Influence of Surface Charge and Protein Intermediary Layer on the Formation of Biomimetic Calcium Phosphate on Silica Nanoparticles. *J. Mater. Chem.* **2012**, *22*, 19562−19569.

(6) Yang, H.; Vovk, G.; Coombs, N.; Sokolov, I.; Ozin, G. A. Synthesis of Mesoporous Silica Spheres under Quiescent Aqueous Acidic Conditions. *J. Mater. Chem.* **1998**, *8*, 743−750.

(7) Destoop, I.; Ghijsens, E.; Katayama, K.; Tahara, K.; Mali, K. S.; Tobe, Y.; De Feyter, S. Solvent-Induced Homochirality in Surface-Confined Low-Density Nanoporous Molecular Networks. *J. Am. Chem. Soc.* **2012**, *134*, 19568−71.

(8) Zhang, X. Y.; Cunningham, M. M.; Walker, R. A. Solvent Polarity at Polar Solid Surfaces: The Role of Solvent Structure. *J. Phys. Chem. B* **2003**, *107*, 3183−3195.

(9) Brindza, M. R.; Walker, R. A. Differentiating Solvation Mechanisms at Polar Solid/Liquid Interfaces. *J. Am. Chem. Soc.* **2009**, *131*, 6207−6214.

(10) Hopkins, A. J.; McFearin, C. L.; Richmond, G. L. Investigations of the Solid−Aqueous Interface with Vibrational Sum-Frequency Spectroscopy. *Curr. Opin. Solid State Mater. Sci.* **2005**, *9*, 19−27.

(11) Mondal, S. K.; Yamaguchi, S.; Tahara, T. Molecules at the Air/Water Interface Experience a More Inhomogeneous Solvation Environment than in Bulk Solvents: A Quantitative Band Shape Analysis of Interfacial Electronic Spectra Obtained by HD-ESFG. *J. Phys. Chem. C* **2011**, *115*, 3083−3089.

(12) Jena, K. C.; Covert, P. A.; Hore, D. K. The Effect of Salt on the Water Structure at a Charged Solid Surface: Differentiating Second- and Third-Order Nonlinear Contributions. *J. Phys. Chem. Lett.* **2011**, *2*, 1056−1061.

(13) Duval, Y.; Mielczarski, J. A.; Pokrovsky, O. S.; Mielczarski, E.; Ehrhardt, J. J. Evidence of the Existence of Three Types of Species at the Quartz-Aqueous Solution Interface at pH 0−10: XPS Surface Group Quantification and Surface Complexation Modeling. *J. Phys. Chem. B* **2002**, *106*, 2937−2945.

(14) Koopal, L. K. Wetting of Solid Surfaces: Fundamentals and Charge Effects. *Adv. Colloid Interface Sci.* **2012**, *179*, 29−42.

(15) Liu, Q.; Yuan, S. L.; Yan, H.; Zhao, X. Mechanism of Oil Detachment from a Silica Surface in Aqueous Surfactant Solutions: Molecular Dynamics Simulations. *J. Phys. Chem. B* **2012**, *116*, 2867−2875.

(16) Manne, S.; Gaub, H. E. Molecular-Organization of Surfactants at Solid−Liquid Interfaces. *Science* **1995**, *270*, 1480−1482.

(17) Tiberg, F.; Jonsson, B.; Tang, J.; Lindman, B. Ellipsometry Studies of the Self-Assembly of Nonionic Surfactants at the Silica Water Interface: Equilibrium Aspects. *Langmuir* **1994**, *10*, 2294−2300.

(18) Brown, M. A.; Huthwelker, T.; Redondo, A. B.; Janousch, M.; Faubel, M.; Arrell, C. A.; Scarongella, M.; Chergui, M.; van Bokhoven, J. A. Changes in the Silanol Protonation State Measured In Situ at the Silica−Aqueous Interface. *J. Phys. Chem. Lett.* **2012**, *3*, 231−235.

(19) Drach, M.; Andrzejewska, A.; Narkiewicz-Michalek, J.; Rudzinski, W.; Koopal, L. K. Theoretical Modeling of Cationic Surfactants Aggregation at the Silica/Aqueous Solution Interface: Effects of pH and Ionic Strength. *Phys. Chem. Chem. Phys.* **2002**, *4*, 5846−5855.

(20) Pokrovsky, O. S.; Golubev, S. V.; Mielczarski, J. A. Kinetic Evidences of the Existence of Positively Charged Species at the Quartz−Aqueous Solution Interface. *J. Colloid Interface Sci.* **2006**, *296*, 189−194.

(21) Sulpizi, M.; Gaigeot, M. P.; Sprik, M. The Silica−Water Interface: How the Silanols Determine the Surface Acidity and Modulate the Water Properties. *J. Chem. Theory Comput.* **2012**, *8*, 1037−1047.

(22) Ong, S. W.; Zhao, X. L.; Eisenthal, K. B. Polarization of Water-Molecules at a Charged Interface—2nd Harmonic Studies of Silica Water Interface. *Chem. Phys. Lett.* **1992**, *191*, 327−335.

(23) Allen, L. H.; Matijevi., E. Stability of Colloidal Silica: Effect of Hydroyzable Cations. *J. Colloid Interface Sci.* **1971**, *35*, 66.

(24) Allen, L. H.; Matijevi., E.; Meties, L. Exchange of Na^+ for Silanolic Protons of Silica. *J. Inorg. Nucl. Chem.* **1971**, *33*, 1293.

(25) Horiuchi, H.; Nikolov, A.; Wasan, D. T. Calculation of the Surface Potential and Surface Charge Density by Measurement of the Three-Phase Contact Angle. *J. Colloid Interface Sci.* **2012**, *385*, 218−224.

(26) Iler, R. K. *The Chemistry of Silica: Solubility, Polymerization, Colloid and Surface Properties, And Biochemistry*; John Wiley & Sons: New York, 1979.

(27) Azam, M. S.; Weeraman, C. N.; Gibbs-Davis, J. M. Specific Cation Effects on the Bimodal Acid−Base Behavior of the Silica/Water Interface. *J. Phys. Chem. Lett.* **2012**, *3*, 1269−1274.

(28) Li, I.; Bandara, J.; Shultz, M. J. Time Evolution Studies of the H_2O/Quartz Interface Using Sum Frequency Generation, Atomic Force Microscopy, And Molecular Dynamics. *Langmuir* **2004**, *20*, 10474−10480.

(29) Dove, P. M. The Dissolution Kinetics of Quartz in Sodium Chloride Solutions at 25 to 300 C. *Am. J. Sci.* **1994**, *294*, 665−712.

(30) Zhao, X. L.; Ong, S. W.; Eisenthal, K. B. Polarization of Water-Molecules at a Charged Interface—2nd Harmonic Studies of Charged Monolayers at the Air−Water Interface. *Chem. Phys. Lett.* **1993**, *202*, 513−520.

(31) Zhao, X. L.; Ong, S. W.; Wang, H. F.; Eisenthal, K. B. New Method for Determination of Surface pKa using 2nd Harmonic Generation. *Chem. Phys. Lett.* **1993**, *214*, 203−207.

(32) Gibbs-Davis, J. M.; Kruk, J. J.; Konek, C. T.; Scheidt, K. A.; Geiger, F. M. Jammed Acid−Base Reactions at Interfaces. *J. Am. Chem. Soc.* **2008**, *130*, 15444−15447.

(33) Green, J. S.; Jorgenson, J. W. Minimizing Adsorption of Proteins on Fused-Silica in Capillary Zone Electrophoresis by the Addition of Alkali-Metal Salts to the Buffers. *J. Chromatogr.* **1989**, *478*, 63−70.

(34) Yakovleva, J.; Davidsson, R.; Lobanova, A.; Bengtsson, M.; Eremin, S.; Laurell, T.; Emneus, J. Microfluidic Enzyme Immunoassay

Using Silicon Microchip with Immobilized Antibodies and Chemiluminescence Detection. *Anal. Chem.* **2002**, *74*, 2994−3004.
(35) Siler, A. R.; Walker, R. A. Effects of Solvent Structure on Interfacial Polarity at Strongly Associating Silica/Alcohol Interfaces. *J. Phys. Chem. C* **2011**, *115*, 9637−9643.
(36) Bloembergen, N. 2ND Harmonic Reflected Light. *Optica Acta* **1966**, *13*, 311−322.
(37) Marowsky, G.; Steinhoff, R.; Chi, L. F.; Hutter, J.; Wagniere, G. 2ND-Harmonic Generation in Quinquethienyl Monolayers. *Phys. Rev. B* **1988**, *38*, 6274−6278.
(38) Eisenthal, K. B. Second Harmonic Spectroscopy of Aqueous Nano- And Microparticle Interfaces. *Chem. Rev.* **2006**, *106*, 1462−1477.
(39) Busson, B.; Tadjeddine, A. Non-Uniqueness of Parameters Extracted from Resonant Second-Order Nonlinear Optical Spectroscopies. *J. Phys. Chem. C* **2009**, *113*, 21895−21902.
(40) Can, S. Z.; Chang, C. F.; Walker, R. A. Spontaneous Formation of DPPC Monolayers at Aqueous/Vapor Interfaces and the Impact of Charged Surfactants. *Biochim. Biophys. Acta* **2008**, *1778*, 2368−2377.
(41) Hiemenz, P. C. *Principles of Colloid and Surface Chemistry*, 2nd ed.; Marcel Dekker, Inc: New York, 1986; Vol. *9*, p 792.
(42) Moridani, M. Y.; Siraki, A.; Chevaldina, T.; Scobie, H.; O'Brien, P. J. Quantitative Structure Toxicity Relationships for Catechols in Isolated Rat Hepatocytes. *Chem.-Biol. Interact.* **2004**, *147*, 297−307.
(43) Iler, R. K. *The Colloid Chemistry of Silica and Silicates*; Cornell University Press: Ithica, NY, 1955.
(44) Benjamin, I. Inhomogeneous Broadening of Electronic Spectra at Liquid Interfaces. *Chem. Phys. Lett.* **2011**, *515*, 56−61.
(45) Mazumder, M.; Bhushan, B. Propensity and Geometrical Distribution of Surface Nanobubbles: Effect of Electrolyte, Roughness, pH, and Substrate Bias. *Soft Matter* **2011**, *7*, 9184−9196.
(46) Yang, J.; Duan, J.; Fornasiero, D.; Ralston, J. Kinetics of CO_2 Nanobubble Formation at the Solid/Water Interface. *Phys. Chem. Chem. Phys.* **2007**, *9*, 6327−6332.
(47) Yang, C. S. C.; Richter, L. J.; Stephenson, J. C.; Briggman, K. A. In Situ, Vibrationally Resonant Sum Frequency Spectroscopy Study of the Self-Assembly of Dioctadecyl Disulfide on Gold. *Langmuir* **2002**, *18*, 7549−7556.
(48) Malin, J. N.; Geiger, F. M. Uranyl Adsorption and Speciation at the Fused Silica/Water Interface Studied by Resonantly Enhanced Second Harmonic Generation and the $\chi^{(3)}$ Method. *J. Phys. Chem. A* **2010**, *114*, 1797−1805.
(49) Steinhurst, D. A.; Owrutsky, J. C. Second Harmonic Generation from Oxazine Dyes at the Air/Water Interface. *J. Phys. Chem. B* **2001**, *105*, 3062−3072.